NATURAL CONVECTION HEAT TRANSFER FROM A HEATED PIPE EMBEDDED IN A LIQUID-SATURATED POROUS MEDIUM

E. F. ATWAN and R.Y. SAKR
Mech. Eng. Dept., Faculty of Eng. (Shoubra), Zagazig University,
108 Shoubra St., Cairo, Egypt

ABSTRACT

A numerical and experimental investigation for natural convection heat transfer from a pipe embedded in a semi-infinite, liquid-saturated porous medium is carried out. The surface of the medium is assumed to be impermeable. The governing equations for Darcy flow are solved using finite element method. The finite element formulation is based on a two-dimension Galerkin approach. Extensive series of numerical solutions are conducted over a wide range of the governing parameters $2\leq h/R\leq 8$, $10\leq Ra\leq 250$, where h/R, and Ra are the burial depth/pipe radius ratio, and the Darcy-Rayleigh number, respectively. The effects of these parameters on both the temperature and flow fields and on the pipe surface heat transfer rate are analyzed. Experiments are conducted on an electrically heated brass pipe buried in a liquid-saturated porous medium enclosed in a vertical container to validate the present predictions. Sand grains with nominal diameter 2.7 mm saturated with water are used as the porous medium. The experimental data are compared with both the present predictions and with those available in the literature and fair agreement is noticed. Correlating equations for the average Nusselt number are obtained as functions of Darcy-Rayleigh number and the pipe burial depth ratio.

KEYWORDS

Natural convection; Porous media; Buried pipe; Darcy-Rayleigh number

1. INTRODUCTION

In recent years, the problem of heat losses from buried pipes in saturated porous medium has received considerable attention. This problem arises, for example, in connection with oil/gas lines where the oil/gas is heated or chilled in order to reduce pumping power, as well as in the context of power plant steam and water distribution lines, underground electrical power transmission lines, thermal insulation of pipes embedded in walls, and burial of nuclear waste.

The early studies that considered the problem of buried pipes and cables assumed the surrounding medium to be purely conductive. Approximate and exact steady-state heat loss calculations are available in the literature [1-8] for pipes and cables with idealized boundary conditions such as isothermal surfaces.

However, in many cases, the medium is permeable to fluid motion. The temperature difference between the pipe and the medium surface may cause natural convection. Consequently, the heat transfer process will consist of natural convection as well as conduction. Generally, the contribution of natural convection to the total heat transfer from buried pipes is as large and, in some cases, larger than the contribution of conduction. Therefore, the problem of heat losses from buried pipes in semi-infinite, saturated, porous medium has been reconsidered lately in order to account for convection. Schroch et al. [9] and Fernandez and Schroch [10] carried out experiments and numerical calculations, using bicylinderical coordinates, for a hot cylinder buried beneath a permeable, horizontal surface. Based on their experimental and numerical results, a heat transfer correlation was suggested, which was later modified by Fernandez and Schroch [10] with an expanded data base.

Farouk and Shayer [11] solved the same problem numerically using a hybird grid system, which involved a polar grid mesh near the cylinder and a cartesian mesh for the remainder of the flow domain. However, their results were significantly different from the predictions of Fernandez and Schroch [10], especially at high Ra values. They attributed this to the fact that the boundary condition that was used along the permeable surface was different between the two studies. Bau [12] considered the problem of a pipe buried beneath a permeable as well as an impermeable, horizontal surface. The cylinder as well as the medium surface were assumed to be maintained at constant temperature. The assumption of a medium surface at constant temperature may be, however, difficult to physically realize for the case of a permeable surface, especially at moderate to high Darcy-Rayleigh number. For low Darcy-Rayleigh number an analytical solution was elegantly obtained for both permeable and impermeable medium surfaces through the use of regular perturbation expansions. Based on the analytical solution that was obtained for the flow and temperature fields, a correlation for Nu was presented for impermeable case which is valid up to an effective Ra, (defined as Ra. h/R) of 60. The validity and range of utility of the correlation were determined through comparisons of the analytical solution to numerical solutions of the full nonlinear equations. It was further shown that an optimal burial depth exists for which the heat losses from the pipe are minimized. Cheng [13] considered the steady natural convection about an isothermal cylinder embedded in an infinite saturated porous medium. Approximate closed-form solutions were obtained for the local as well as the average Nusselt number by applying boundary layer approximations similar to those that are applied to the classical boundary layer theory. The applicable boundary layer equations were solved using the similarity technique as well as the Pohlhausen integral method. Although the two solutions, in terms of the average Nusselt number, are similar in form, they differ on the numerical constants. Himasekhar and Bau [14] extended the work presented for the impermeable case by Bau [12] to include a convection boundary condition at the medium's surface. An analytical solution was obtained for both hot and cold pipes by constructing a double perturbation expansion in terms of Darcy-Rayleigh and inverse of Biot numbers. A correlation was presented for Nu as a function of the burial depth, and the Bi Ra. The validity of the correlation was, once again, established by comparison with numerical results of the full nonlinear equations. An optimal burial depth was found to also exist for surfaces with convective boundary conditions. Facas [15] presented a study for the natural convection heat transfer from a pipe with two baffles attached along its surface buried beneath a semi-infinite, saturated, porous medium. The surface of the medium is assumed to be permeable. The complicated geometry is handled through the use of a body-fitted curvilinear coordinate system. The solution to the fluid flow and temperature field has been obtained numerically using finite difference method. Results were presented for three baffle lengths and a range of burial depths and Darcy-Rayleigh numbers. His analysis showed that substantial energy savings could be realized if baffles are used.

The problem of underground power transmission cables attracts the interest of many investigators [16-18]. Yeh and Chang [17] carried out an experimental study to investigate the optimum eccentricity of the power cable inside an underground conduit to adjust level of the maximum temperature decrement. Their results showed that natural convection enhancement was achieved by eccentricity of power cable.

Recently, the effect of permeability of the backfill layer around pipes or cables and groundwater advection are investigated experimentally and numerically [19-27]. For example, Nago and Lai [20] examined numerically natural convection from a buried pipe with a layer of backfill. They investigated how a change in the permeability of the backfill would affect the flow patterns and heat transfer results. The parameters studied in their investigation are Darcy-Rayleigh number, permeability ratio, and the backfill thickness. Their results suggested that a more permeable backfill could minimize the heat loss and confine the flow to a region close to the pipe.

From the above review, it can be concluded that most of the previous investigations deal the problem of heat loss from a buried pipe in a semi-infinite, saturated, permeable medium were based on the conduction models and few of these studies introduced the natural convection. Also, these works are limited to small values of Darcy-Rayleigh numbers. So, the objective of the present work is to develop numerically a general model, validated by an experimental work, capable of handling the most important heat transfer parameters and practical variables in the field of buried pipe lines in order to achieve the optimum working conditions.

2. NUMERICAL ANALYSIS

2.1 Assumptions and Model Equations

The problem considered in the present study is a pipe with radius R buried at a distance h beneath a horizontal impermeable surface of a semi-infinite, saturated porous medium as shown in Fig. (1-a), where h represents the vertical depth of the cylinder center from the impermeable upper surface. The surface of the pipe is assumed to be maintained at a constant temperature T_w , whereas the top horizontal impermeable surface is maintained at a constant temperature T_o with $T_w>T_o$. A rectangular flow domain is approximated for obtaining the numerical solutions. The governing equations for steady-state natural convection with the Boussinesq, Darcy flow, and negligible inertia approximations are given as [11]:

Continuity:

$$\nabla.\vec{v} = 0 \qquad (1)$$

Momentum:

$$\frac{\mu}{K}\vec{v} = -[\nabla p - \rho_f \vec{g}] \qquad (2)$$

Energy:

$$(\rho c)_f \frac{\partial T}{\partial t} = k_e \nabla^2 T - (\rho c)_f [\nabla.\vec{v}\, T] \qquad (3)$$

where the subscript e indicate equivalent properties for the medium. The density in the buoyancy term in equation (3) is related to the temperature by a linear equation of state:

$$\rho_f = \rho_o \left[1 - \beta_f (T - T_o)\right] \qquad (4)$$

where ρ_o s the density at a reference temperature T_o and β_f is the coefficient of thermal expansion, defined as:

$$\beta_f = -\frac{1}{\rho_o}\left(\frac{\partial \rho}{\partial T}\right)_P \qquad (5)$$

The other symbols appearing in equations (1)-(5) are defined in the nomenclature.
By taking the curl of equation (2) and using the equation of state (4), we obtain the following equations:

Momentum:

$$\nabla^2 \psi = -\frac{K}{\mu} g\, \rho_o \beta_f \frac{\partial T}{\partial x} \qquad (6)$$

Energy:

$$\nabla^2 T - \frac{\rho_f c_f}{k_e}\left[\frac{\partial\psi}{\partial y}\frac{\partial T}{\partial x} - \frac{\partial\psi}{\partial x}\frac{\partial T}{\partial y}\right] = \frac{\rho_f c_f}{k_e}\frac{\partial T}{\partial t} \tag{7}$$

It must be noted in the above two equations that the velocity components are defined in terms of the stream function (ψ) as;

$$u = \frac{\partial\psi}{\partial y}, \quad v = -\frac{\partial\psi}{\partial x}$$

2.2 Dimensionless Governing Equations

Before undertaking a numerical solution, the first step should invariably be to place the equations to be solved in a dimensionless form having as few parameters as possible. This may be accomplished for equations (6)-(7) by introducing the following dimensionless variables:

$$\theta = \frac{T - T_o}{T_w - T_o}, \quad x^* = \frac{x}{R}, \quad y^* = \frac{y}{R}, \quad \psi^* = \frac{\psi}{\alpha\rho_f}, \quad \tau = \frac{k_e}{(\rho c)_e}\frac{t}{R^2}$$

where α is the effective (equivalent) thermal diffusivity of the porous medium defined as:

$$\alpha = \frac{k_e}{(\rho c)_f}$$

The resulting dimensionless governing equations reduce to:

$$\nabla^2\psi^* = -Ra\frac{\partial\theta}{\partial x^*} \tag{8}$$

$$\nabla^2\theta - \left(\frac{\partial\psi^*}{\partial y^*}\frac{\partial\theta}{\partial x^*} - \frac{\partial\psi^*}{\partial x^*}\frac{\partial\theta}{\partial y^*}\right) = \frac{\partial\theta}{\partial\tau} \tag{9}$$

The Darcy-Rayleigh number (Ra) based on the pipe radius R is defined as

$$Ra = \frac{g\rho_f\rho_r\beta_f c_f R(T_w - T_o)}{k_e(\mu/K)}$$

2.2.1 Solution domain and boundary conditions

Because of the geometry considered, a vertical symmetry plane exists and the problem is solved only for the vertical half plane. Also, since the coupled set of elliptic governing equations can be solved only if the conditions are specified along the entire boundary that closes the flow field. The pipe is considered to be held at a uniform temperature T_w and the upper surface is considered to be impermeable and isothermal. Moreover, since it is difficult to treat an infinite domain numerically, the physical domain will be truncated by assuming that the two far boundaries at infinite x* and negative infinite y* are at a large distance (w/R) and (d/R) away from the center of the pipe, respectively. Approximate values for (w/R) and (d/R) that lead to solutions that are independent of the value set for these two quantities can be selected only through numerical experimentation.

The boundary conditions are handled as follows:

a) Along the symmetry plane:

$$\psi^* = 0, \quad \frac{\partial\theta}{\partial x^*} = 0 \tag{10-a}$$

b) At the pipe surface:

$$\psi^* = 0\,, \quad \theta = 1.0 \tag{10-b}$$

c) At the upper (top) surface:

$$\psi^* = 0\,, \quad \theta = 0 \tag{10-c}$$

d) At the far field boundaries:

It is assumed that if the far field boundaries are set sufficiently far away (given by w and d in Fig. 1) from the center of the pipe, then the velocity components in the direction parallel to far field surfaces is negligible. i.e.

$$\begin{aligned} &\textit{At}\ \text{the far bottom surface}\ (y^* = -d/R): \quad && \frac{\partial \psi^*}{\partial y^*} = 0, \quad \frac{\partial \theta}{\partial y^*} = 0 \\ &\text{At the far right surface}\ \ (x^* = w/R): && \frac{\partial \psi^*}{\partial x^*} = 0, \quad \frac{\partial \theta}{\partial x^*} = 0 \end{aligned} \tag{10-d}$$

2.3 Heat transfer

The local Nusselt number along the pipe surface is defined as:

$$Nu_\gamma = -\left(\frac{\partial \theta}{\partial n}\right)_{x^{*2}+y^{*2}=1} \tag{11}$$

where n represent the direction normal to the pipe surface.

The mean or average value of Nusselt number at the pipe surface is given by:

$$\overline{Nu} = \frac{1}{\pi}\int_0^\pi Nu(\gamma)\, d\gamma \tag{12}$$

and the integration was carried out using Simpson's rule.

2.4 Method of Solution

The solution of Eqs. (8) and (9) subject to the boundary conditions specified by Eq. (10) is obtained numerically by using the Galerkin based finite element method [28, 29]. The objective of the finite element is to transform the system of governing equations into a discretized set of algebric equations. The procedure begins with the division of the continuum region of interest into a number of simply shaped regions called elements. The grid used in the present calculation is illustrated in Fig. (1-b).

2.4.1 The finite element formulation

The type of the used elements is linear triangular elements. For simplicity, the "*" which is used for the dimensionless x, y, and ψ is omitted in the following equations. The stream function and the temperature in an element can be represented in terms of nodal stream function and temperature by simple polynomials:

$$\psi^e = \sum_{m=1}^{3} N_m \psi_m \tag{13-a}$$

$$\theta^e = \sum_{m=1}^{3} N_m \theta_m \tag{13-b}$$

where;

$$N_1 = \frac{1}{2A}\ (a_1 + b_1\, x + c_1\, y) \tag{14-a}$$

$$N_2 = \frac{1}{2A}\,(a_2 + b_2 x + c_2 y) \qquad (14\text{-b})$$

$$N_3 = \frac{1}{2A}\,(a_3 + b_3 x + c_3 y) \qquad (14\text{-c})$$

A = area of the triangle 123

where;

$a_1 = x_2y_3 - x_3y_2$ $\quad$ $a_2 = x_3y_1 - x_1y_3$ $\quad$ $a_3 = x_1y_2 - x_2y_1$

$b_1 = y_2 - y_3$ $\quad$ $b_2 = y_3 - y_1$ $\quad$ $b_3 = y_1 - y_2$

$c_1 = x_3 - x_2$ $\quad$ $c_2 = x_1 - x_3$ $\quad$ $c_3 = x_2 - x_1$

The interpolation functions $[N_1, N_2, N_3]$ in Eq. (14) are derived from an assumption of linear variation of stream function and temperature in the element. The approximate expressions of the system variables ψ^e and θ^e are substituted into the governing equations, Eqs. (8) and (9), and the global errors are minimized using the above interpolation functions N_i (i = 1, 2, 3) as a weighting functions. The solution of Eqs. (8) and (9) that satisfy the boundary conditions, Eq.(10), can be written after weighted integration over the domain Ω^e and the application of Green's theorem, in the equivalent matrix form as:

$$[K_1]\{\theta\} = \{F_1\} \qquad (15\text{-a})$$

$$[K_2]\{\psi\} = \{F_2\} \qquad (15\text{-b})$$

where,

$$[K_1] = \sum_{e=1}^{E} \int_{\Omega^e} \left(\frac{\partial [N]^T}{\partial x}\cdot\frac{\partial [N]}{\partial x} + \frac{\partial [N]^T}{\partial y}\cdot\frac{\partial [N]}{\partial y}\right) d\Omega^e + \sum_{e=1}^{E} \int_{\Omega^e} \left(\psi_y [N]^T\cdot\frac{\partial [N]}{\partial x} - \psi_x [N]^T\cdot\frac{\partial [N]}{\partial y}\right) d\Omega^e$$

$$\{F_1\} = \sum_{e=1}^{E} \int_{\Gamma^e} \left([N]^T \frac{\partial N}{\partial x} + [N]^T \frac{\partial N}{\partial y}\right) d\Gamma^e$$

$$[K_2] = \sum_{e=1}^{E} \int_{\Omega^e} \left(\frac{\partial [N]^T}{\partial x}\cdot\frac{\partial [N]}{\partial x} + \frac{\partial [N]^T}{\partial y}\cdot\frac{\partial [N]}{\partial y}\right) d\Omega^e$$

$$\{F_2\} = \sum_{e=1}^{E} \int_{\Gamma^e} [N]^T \frac{\partial [N]}{\partial x} d\Gamma^e + \int_{\Gamma^e} [N]^T \frac{\partial [N]}{\partial y} d\Gamma^e + \sum_{e=1}^{E} \int_{\Omega^e} Ra\,\theta [N]^T \frac{\partial [N]}{\partial x} d\Omega^e$$

where;

E = total number of elements, Ω bounded domain, Γ domain boundary, and

$$\Psi_x = \frac{\partial \psi}{\partial x}, \quad \Psi_y = \frac{\partial \psi}{\partial y}$$

The resulting finite element algebric equations are solved iteratively using the method of successive overrelaxation (SOR) through a computer code written in FORTRAN langauge.

The iterative procedure was terminated when the following relative convergence criterion was satisfied for both the stream function and the temperature:

$$\left|\frac{\psi^{n+1}-\psi^{n}}{\psi^{n+1}}\right| \; ; \quad \left|\frac{\theta^{n+1}-\theta^{n}}{\theta^{n+1}}\right| \leq \delta$$

where, δ was assigned the value 10^{-4} since the use of a more stringent condition did not make any significant difference in the solution.
Since as mentioned previously, the numerical results for the problem under consideration will, in general, be sensitive to the values for (w/R) and (d/R). As a result, for different values of h/R and Darcy-Rayleigh number, minimum values for (w/R) and (d/R) has to be determined such that the mean Nusselt number would be independent of these two parameters. The values of 7 and 12 for (d/R) and (w/R), respectively, were found to be adequate for the range of Darcy-Rayleigh number and h/R investigated.

3. EXPERIMENTAL INVESTIGATION

3.1 Experimental Apparatus and Instrumentation

An experimental apparatus consists mainly of a porous media container and brass tube instrumented with electric heater is constructed. The container is constructed from galvanized steel sheet 1 mm thick and holds the saturated porous medium and the hot pipe. The test section has approximate dimensions of 300 × 300 × 350 mm (length, width, height, respectively) to cover the values of (d/R) and (w/R) of 7 and 12, respectively. The embedded pipe is a brass tube of 22 mm outer diameter and 6 mm thick. The surface temperature of the heated pipe was measured by six calibrated 0.5 mm teflon insulated alumel-chromel (K type) thermocouples. The thermocouples were located in longitudinally machined grooves (2.5mm x 2.5 mm) made through the outside surface of the tube and distributed angularly along the pipe wall as shown in Fig. (2-a&b). All thermocouple junctions were embedded close to the outer surface of the pipe wall and the lead wires were taken from one end of the tube. The slots are then filled with brass powder mixed with epoxy and then sanded to give a smooth surface.

The horizontal top cover is made of 1 mm thick galvanized steel sheet which is impermeable to meet the numerical model assumptions. This upper cover is removable so that the porous medium can be easily placed in the test section. Forty alumel-chromel (K type) thermocouples are used to measure the temperature distribution in the porous media along the vertical symmetrical plane. These thermocouples are fixed on a holding plastic screen and then placed in the test apparatus before its filling with porous medium.

The porous media used in the experiments is sand grains having an average diameter of 2.7 mm. The thermal conductivity of the sand grains is 1.83 W/m K. The sand "grains" are, in fact, not exactly spherical but have a narrow size distribution for which the equivalent diameter is determined from the lower and upper limits of the DIN standard sieving analysis. The porosity was estimated by measuring the volume of water that needed to fill the particles void space in cylindrical container of known volume. The porosity (ε) of the system filled with 2.7 mm beads is 0.381. The corresponding permeability calculated from Kozeny-Carmen equation [24] as:

$$K = \frac{\varepsilon^{3}\, d_p^{2}}{180(1-\varepsilon)^{2}} \tag{16}$$

is 0.4851×10^{-8} m^2.

The heater used for heating the brass tube is ready-made heater of total resistance 90 ohm with stainless steel sheath of outer diameter 10 mm and length of 32 cm which is fitted into the brass tube. The heater ends are supported on the container wall through ceramic sleeves. A voltage regulator of output voltage varies from 0 to 250 Volt is used to provide and control the power input to the heater. The power input to the heater is estimated by measuring the voltage drop across the heater using a digital multi-meter (one decimal point) and the known resistance of the heater, which is measured by the same multi-meter. All thermocouples used in the present experimental study are calibrated prior to their installation in the apparatus. These thermocouples are wired into a thermocouple selector switch which is connected to a digital compensating thermometer able to read temperature to one tenth of a degree Celsius.

3.2 Experimental Procedures

The burial depth of the pipe is first specified and then the pipe with the thermocouples screen holder are fixed in the galvanized steel container. The fine fiberglass screen holder of mesh size slightly smaller than the diameter of the sand beads. It is believed that the screen has a negligible influence on the flow and heat transfer through the porous media. The sand beads were poured carefully inside the container until it was filled. Then, the water was carefully siphoned into the test section to ensure that no air was trapped in the matrix or to prevent air from mixing with the saturating fluid.

Power was supplied to the heater and adjusted to give a certain heat flux corresponding to a specified Darcy-Rayleigh number. The steady state was obtained before recording the thermocouples readings and the power supplied for any experimental run. In general, 5 to 8 hours was required to get one set of data. For the present experiments, the maximum variation on the hot pipe wall from a mean value was 4.0 percent.

3.3 Data Reduction

An important property of the porous medium is the effective thermal conductivity, which was calculated by using the following typical mixing rule [31]:

$$k_e = \varepsilon k_f + (1-\varepsilon) k_s \tag{17}$$

Another important property of the porous medium is the permeability, which is calculated using Eq.(16). The Darcy-Rayleigh number (based on the pipe radius R) is calculated from the definition:

$$Ra = \frac{g\beta_f KR(T_w - T_\infty)}{\upsilon\alpha} \tag{18}$$

It may be noted that all fluid properties, which used in the calculation of the experimental results are calculated at a temperature which is the arithmetic mean of the pipe wall mean temperature (T_w) and the far away temperature (T_∞) as:

$$T_m = \frac{(T_w + T_\infty)}{2} \tag{19}$$

The average Nusselt number on the heated pipe surface based on the pipe radius, R, is calculated from the definition:

$$\overline{Nu} = \frac{\bar{h}\, R}{k_e} \tag{20}$$

where, h is the average heat transfer coefficient and given by

$$\bar{h}_i = \frac{[\text{power input to the heater - losses}]}{(\text{pipe outer surface area}) \times (\text{temperature difference})} \tag{21}$$

The losses were estimated by calculating the conduction through the two ends of the heater.

Error analysis, including that in temperature measurements and the fluid properties, shows that the Nusselt number has an uncertainty of 4.5 percent and the Darcy-Rayleigh number is uncertain by up to 5.6 percent of the reported values.

4. RESULTS AND DISCUSSION

The accuracy of the numerical procedure employed in the present study was tested through comparison of the present predictions with those reported in the literature for the case of natural convection of two concentric horizontal cylinders with radius ratio of 2. The results obtained using the present code is in fair agreement with the others [15, 32-35], as shown in Table 1.

Some representative numerical results are first obtained and presented to illustrate the effect of the various governing parameters, the Darcy-Rayleigh number (Ra) and burial depth ratio (h/R) on natural convection from a pipe buried in a semi-infinite, saturated porous medium.

4.1 Flow and Temperature Fields

Figure (3) shows the computed steady-state streamlines and isotherms with the aid of the present numerical scheme for a pipe buried at a depth ratio (h/R) of 2 for values of the Darcy-Rayleigh number (Ra) ranging from 10 to 250. Inspection of these maps show that, when the inner cylinder is heated at a moderate Darcy-Rayleigh number (Ra=10), the fluid adjacent to the pipe becomes hotter and thus tends to rise until it hits the top, cold surface. As the fluid travels along the cold, horizontal surface, it cools down and eventually descends to form a circulatory convective cell. The flow consists of a single cell filling the entire half domain and rotating slowly in the clockwise direction (counter clockwise in the other half). Figure (3) shows also that, for Ra=10, the isotherms exhibit minimal distribution from a pure conduction solution (Ra=0) indicating that the conduction is the dominant mode of heat transfer and weak convective effects. This can be noticed through the uniform isotherms around the pipe and the substantially thick boundary layer around the pipe. The flow cell is small and has a center at a level of the pipe centerline. However, as Darcy-Rayleigh number increases (Ra>10), the vortex or central flow point is shifted noticeably above the level of the pipe centerline and the flow cell becomes larger and a much more vigorous convective flow is indicated by the higher values of the streamlines. The thermal boundary layer is much thinner due to increasing the fluid velocity. Also, the isotherms become increasingly skewed in the upward direction which results from the relatively strong convective flow. The same behavior is noticed for burial depth ratio of 4, 5, 6 and 8 (not included here for brevity).
Finally, Fig. (4) depicts the streamlines and isotherms for Ra=150 and different values of burial depth ratio (h/R) ranging from 2 to 8. Inspection of this figure shows that as the burial depth ratio increases the convective flow increases indicated by the higher values of the

Table 1: Comparison of the average Nusselt number for natural convection between two concentric horizontal cylinders with a radius ratio of 2.

	Facas [15]	Caltagirone [32]	Facas & Farouk [33]	Bau [34]	Rao et al. [35]	Present Code
Grid size	50x50	49x49	25x25	30x44	10x10	10x18
Ra=50	1.342	1.328	1.362	1.335	1.341	1.317
Ra=100	1.835	1.829	1.902	1.844	1.861	1.865

stream function and a thin boundary layer forms near the cylinder surface due to increasing the fluid velocity. Also, it can be seen from Figs. (3) and (4) that the flow near the cylinder is much stronger compared to the rest of the flow domain.

4.2 Heat Transfer Results

For a horizontal heated cylinder submerged in an unbounded medium, the natural convection heat transfer characteristics are functions of the Darcy-Rayleigh number only [11]. While if the cylinder is buried in a semi-infinite medium in close proximity to the upper bounding surface, the Nusselt number becomes dependent of the geometry as well, in particular of the burial depth. To study the effects of h/R ratio on the heat transfer characteristics, computational results were obtained for h/R values of 2, 3, 4, 5, 6, 7, and 8 for Darcy-Rayleigh numbers (based on the radius of the pipe) varying from 10 to 250. Figure (5a-c) shows the predicted local Nusselt number for a wide range of Darcy-Rayleigh number, for burial depths, h/R, of 3, 5 and 8, respectively. It is noticed from the figure that the local Nusselt numbers are high at the bottom region of the pipe. This is due to little fluid movement in this region. For all the investigated Darcy-Rayleigh numbers, the local Nusselt number decreases continuously reaching a minimum at the top of the pipe. Also, the increased burial depth (from h/R of 3 to 5 to 8) causes an increase in the local Nusselt numbers, especially at lower stagnation regions (γ<60 deg.). It is also noticed that at the same circumferential angle, as Darcy-Rayleigh number increases the local Nusselt number increases.

The steady-state numerical results of the average Nusselt numbers for various h/R ratios and for the entire Darcy-Rayleigh number range (50-250) are shown in Fig.(6). It is noticed from the figure that, at the same Darcy-Rayleigh number as the burial depth ratio increases the average Nusselt number increases till h/R= 6 and any more increase in burial depth ratio leads to a slight increase in the average Nusselt number, approaching asymptotically a value which corresponds to the value associated with a pipe buried in an infinite medium. This behavior is consistent with the thermal and flow fields presented before. Also, the variation of the average Nusselt number with Darcy-Rayleigh number at different burial depths is shown in Fig. (7). The figure shows that the increase in Darcy-Rayleigh number leads to an increase in the average Nusselt number for all burial depth ratios.

4.3 Comparison of Predictions with Experiments

The present experimental heat transfer results are compared with the present model predictions for a wide range of the governing parameters as shown in Fig.(7). It is clear from the figure that numerical values for the average Nusselt number are in fair agreement with the experimental values especially for higher values of Darcy-Rayleigh number. The maximum deviation is 30 percent. In reality, the discrepancies between the experimental and the predicted average Nusselt number is attributed to the differences in considering the upper bounding thermal boundary condition, which is assumed to be isothermal in the numerical solution as discussed earlier.

4.4 Nusselt Number Correlation

Based upon the numerical heat transfer results, a general correlation that accounts for the governing parameters was developed by expressing the average Nusselt number on the heated wall of the buried pipe as a function of the governing dimensionless groups as:

$$\overline{Nu} = a\, Ra^{b} \left(h/R\right)^{c} \tag{22}$$

where a, b, and c are the empirical constants and obtained from the least-squares fitting of the numerical data. Using a least-squares approach, the values of the constants a, b, and c are 0.266, 0.282, and 0.182, respectively. Therefore, the general form of the empirical correlation for the present numerical heat transfer results is:

$$\overline{Nu} = 0.266\,Ra^{0.282}\,(h/R)^{0.182} \tag{23}$$

This correlation is valid for the following range of parameters:

$10 \le Ra \le 250$, and $2 \le h/R \le 8$

where the average Nusselt number and the Darcy-Rayleigh number are based on the pipe radius R. The predicted values using Eq. (23) are within ±8 percent of the computed ones for about 80 percent of the predicted data. The deviations between the predicted and computed numerical values are mainly due to the continuous change in the slope of Nu vs. Ra and Nu vs. h/R curves. A further subdivision of the data may be results in a significant improvement in the mean deviation of the correlation.

A similar correlation is obtained for the experimental results in the form:

$$\overline{Nu} = 0.376\,Ra^{0.168}\,(h/R)^{0.284} \tag{24}$$

This correlation is valid for the following range of parameters:

$5 \le Ra \le 92$, and $2 \le h/R \le 8$

with a maximum deviation of ±13 percent.

Also, the present experimental correlation over-predicts the average Nusselt number by a maximum value of 30 percent than the numerical one as shown in Fig.(8).

5. CONCLUSIONS

The natural convection from a pipe buried in a semi-infinite saturated porous medium, was investigated, numerically and experimentally. The following conclusions are drawn from the present numerical and experimental data.

1. The behavior of the average Nusselt number as a function of burial depth to pipe radius ratio is found to be quite different for conduction and convection-dominated cases.
2. The increase of Darcy-Rayleigh number leads to an increase in the average Nusselt number at all burial depths ratios due to the dominant-convection mode.
3. The average Nusselt number increases with the increase in the burial depth ratio.
4. The local Nusselt number decreases continuously from the bottom of the pipe to its top due to fluid movement in this region..
5. A fair agreement is noticed between the present numerical and experimental results, where the present numerical model under-predicts the average Nusselt number by a maximum value of 30 percent compared with experimental data.
6. Two correlating equations for the average Nusselt number as a function of the Darcy-Rayleigh number and the burial depth ratio are obtained based on the present experimental data as well as the predictions.

NOMENCLATURE

SI units were applied for the whole parameters used in this paper.

A	area of the linear triangular element
C	specific heat
D	distance between the pipe center and bottom of the solution domain
d_p	particle diameter
g	gravity vector
h	burial depth
$\bar{h}$	average heat transfer coefficient
K	Permeability
k	thermal conductivity
Nu	Nusselt number
N	interpolation function
n	normal direction or iteration No.
p	pressure
R	pipe radius
Ra	Darcy-Rayleigh number
T	temperature
v	velocity vector
w	width of the solution domain
x, y	cartesian coordinates

Greek symbols

α	thermal diffusivity
β	coefficient of thermal expansion
γ	circumferential angle
θ	dimensionless temperature
ε	porosity
τ	dimensionless time
μ	viscosity
ρ	density
ψ	stream function

Subscripts

e	effective
f	fluid
o	reference
w	wall surface

Superscripts

p	current iteration
p-1	previous iteration
–	average value
*	dimensionless

REFERENCES

1- Lebedev, M. N., Skalakaya, I. P. and Ufyland, Y. S., Worked Problems in Applied Mechanics, Dover, New York, 1979.

2- Thiyagarayan, R. and Yovanovich, M.N., “Thermal Resistance of a Buried Cylinder with Constant Heat Flux Boundary Condition”, J. Heat Transfer, Vol. 96, pp. 249-255, 1974.

3- Eckert, E. R. G. and Drake, R. M., Analysis of Heat and Mass Transfer, Mc-Graw Hill, New York, 1972.

4- Bau, H. H. and Sadhal, S. S., “Heat Loss From a Fluid Flowing in a Pipe”, Int. J. Heat Mass Transfer, Vol. 25, pp.1621-1629, 1982.

5- Himasekhar, K. and Bau, H. H., “Thermal Convection Associated with Hot/Cold Pipes Buried in a Semi-infinite, Saturated, Porous Medium”, Int. J. Heat Mass Transfer, pp. 263-273, 1987.

6- Martin, W. W. and Sadhal, S., “Bounds on Transient Temperature Distribution due to a Buried Cylindrical Heat Source” , Int. J. Heat Mass Transfer, Vol. 21, pp. 783-789, 1978.

7- Neigiz, A., Hastaglu, M. A. and Heidemann, R. A. “Three Dimensional Transient Heat Transfer from a Buried Pipe. I- Laminar Flow”, Chem. Eng. Science, Vol. 48, pp. 3507-3517, 1993.

8- Abdel-Hadi E. A, Abel-Azim, A. A, and Sakr R.Y., “Transient Heat Transfer From A Fluid Flowing in a Buried Pipe”, Engng. Res. Jour., Helwan University, Faculty of Engng., Vol. 4, pp. 212-230, April, 1995.

9- Schrock, V. E., Fernandez, R.T. and Kesvan, K. “Heat Transfer from Cylinders Embedded in a Liquid Filled Porous Medium”, Proc. Int. Heat Transfer Conf., Paris, Vol. VII, CT3-6, 1970.

10- Fernandez, R.T. and Schrock, V. E., “Natural Convection from Cylinders Buried in a Liquid Saturated Porous Medium”, Proc. of the Int. Heat Transfer Conf., Munich, pp.335-340, 1982.

11- Farouk, B and Shayer, H., “Natural Convection Around a Heated Cylinder in a Saturated Porous Medium”, ASME J. Heat Transfer, Vol. 110, 1988.

12- Bau, H.H., “Convective Heat Losses From a Pipe Buried in a Semi-Infinite Porous Medium”, Int. J. of Heat Mass Transfer, Vol. 27, No. 11, pp. 2047-2056, 1984.

13- Cheng, P. “Natural Convection in a Porous Medium: External Flows", Presented at NATO Advanced Study Institute, July 16-27, 1984.

14- Himasekhar, K. and Bau, H. H. "Thermal Convection Associated with Hot/Cold Pipes Buried in a Semi-Infinite, saturated Porous Medium", Int. J. Heat Mass Transfer, No. 2, pp. 263-273, 1987.
15- Facas, G. N., "Natural Convection From a Buried Pipe with External Baffles", Numerical Heat Transfer, Part A, No.27, pp. 595-609, 1995.
16- Anders, G. J., "Rating of Cables on Riser Poles, in Trays, in Tunnels and Shafts"", IEEE Transactions on Power delivery, Vol. 11, No.1, pp. 3-10, 1996.
17- Yeh, Chun-Lang, Chang, Keh-Chin, "Enhancement of Natural Convection by Eccentricity of Power Cable Inside Underground Conduit", J. of Thermophysics & Heat Transfer, Vol. 14, No.4, pp. 604-606, 2000.
18- Chakir, A. S., Aquelet, M. N., "Study of a Turbulent Natural Convection in Cylindrical Annuli of Gas-Insulated Transmission Lines 400 kV", Applied Thermal Engineering, Vol. 23, No.10, pp.1197-1208, 2003.
19- Alkam, M. K., Al-Nimr, M. A., "Solutions for Classical Fluid Flow Problems in Porous Domains", JSME International Journal, Series B, Vol. 42, No.2, pp. 206-213, 1999.
20- Ngo, C. C., Lai, F. C., "Natural Convection From a Pipe Buried in a Porous Medium With Variable Permeability", ASME, Heat Transfer Division, HTD, Vol. 374, pp. 349-355, 2003.
21- Hassanien, I. A., Salama, A. A., and Elaiw, A. M., "Variable Permeability Effect on Vortex Instability of Mixed Convection Flow in a Semi-Infinite Porous Medium Bounded by a Horizontal Surface", Applied Mathematics & Computation, Vol. 146, pp. 829-847, Dec. 2003.
22- Nairen D., Qinyu L., and Zhadohong F., "Heat Transfer in Ground Heat Echangers With Groundwater Advection", Int. J. of Thermal Sciences, Vol. 43, pp. 1203-1211, 2004.
23- Choudhary, M. K., Karki, K. C., and Patanker S.V., "Mathematical Modeling of Heat Transfer, Condensation, and Capillary Flow in Porous Insulation on a Cold Pipe", Int. J. Heat Mass Transfer, Vol. 30, pp. 5629-5638, 2004.
24- Nield D. A. and Kuznetstov, "Forced Convection in a Bi-Disperse Porous Medium Channel", Int. J. Heat Mass Transfer, Vol. 47, pp. 5375-5380, 2004.
25- Aldoss, T. K., Alkam, M. and Shatarah, M., "Natural Convection From a Horizontal Annulus Partially Filled With Porous Medium", Int.Comm. Heat Mass Transfer, Vol. 31, no. 3, pp. 441-452, 2004.
26- Saeid, N. H. and Pop, I., "Non-Darcy Natural Convection in a Square Cavity Filled With a Porous Medium", Fluid Dynamics Research, Vol. 36, pp. 35-43, 2005.
27- Mahmud, S. and Fraser, R. A., "Flow, Thermal, and Entropy Generation Characteristics Inside a Porous Channel With Viscous Dissipation", Int. J. of Thermal Sciences, Vol. 44, pp. 21-32, 2005.
28- Rao, S. S., The Finite Element Methods in Engineering, Pergamon Press, 1982.
29- Pepper, D. W., and Heinrich, J.C., The Finite Element Method- Basic Concepts and Applications, Hemisphere Publishing Corporation, 1992.
30- Bear, J., Dynamics of Fluids in Porous Media, Elsevier, New York, 1972.
31- Atwan, E. F., El-Shazly, K. M., Khalil, E. E., and Abdel-Salam, M. S., "Numerical and Experimental Investigation of Natural Convection in Vertical Annular Porous Layer," Proc. of the 1st Jordanian Mechanical Engineering Conference, Amman , Vol. 2, pp. 491-524, 1995.
32- Caltagirone, J. P. "Thermoconvective Instabilities in a Porous Medium Bounded by Two Concentric Horizontal Cylinders", J. of Fluid Mechanics, Vol. 76, pp. 337-362, 1976.
33- Facas, G.N and Farouk, B. "Transient and Steady State Natural Convection in a Porous Medium Between Two Concentric Cylinders", ASME J. Heat Transfer, Vol. 105, pp. 660-663, 1983.
34- Bau, H.H. "Thermal Convection in a Horizontal, Eccentric Annulus Containing a Saturated Porous Medium- An Extended Perturbation Expansion", Int. J. Heat Mass Transfer, Vol. 27, pp. 2277-2287, 1984.
35- Rao, Y. F, Fukuda, K. and Hasegawa, S. "Steady and Transient Analyses of Natural Convection in a Horizontal Porous Annulus with the Galerkin Method", ASME J. Heat Transfer, Vol. 109, pp. 919-927, 1987.

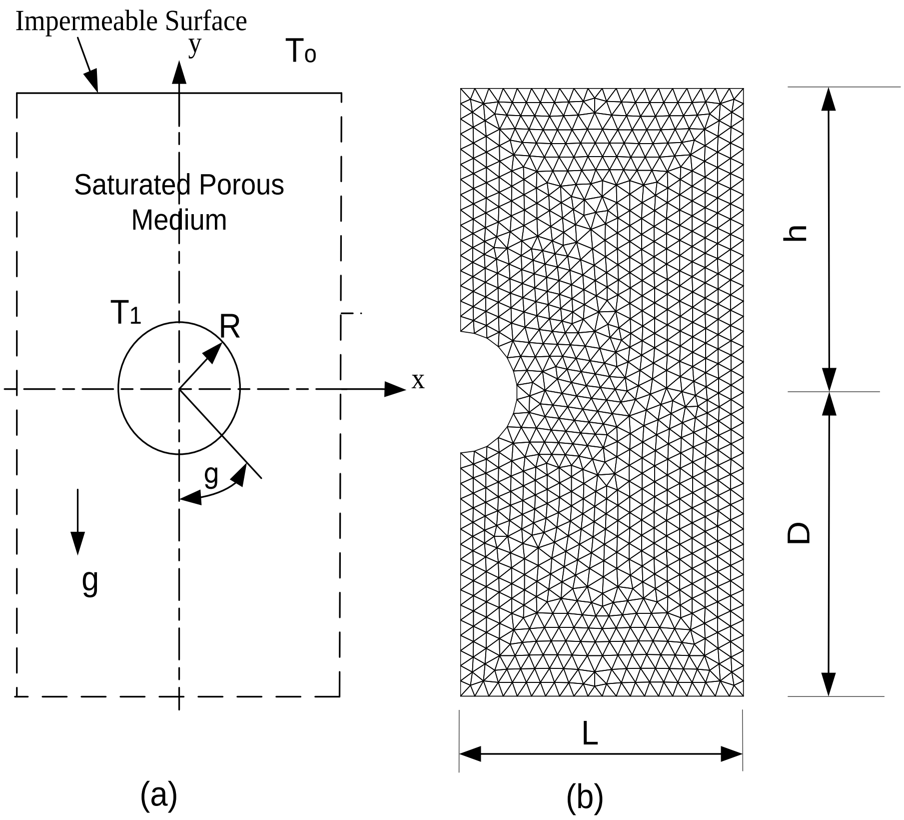

Fig. (1) Problem geometry and mesh generation used in the present code

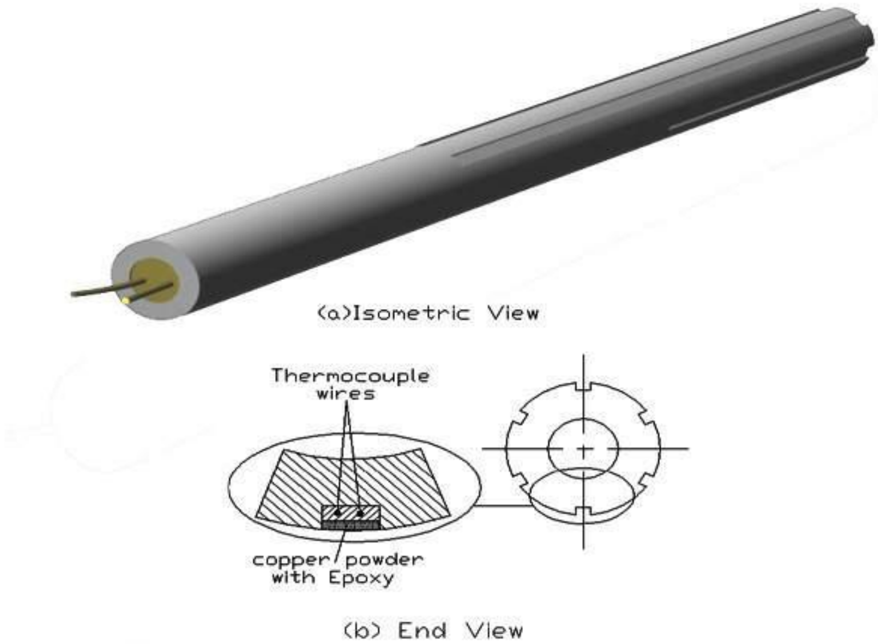

Fig. (2): The buried brass pipe with heating element

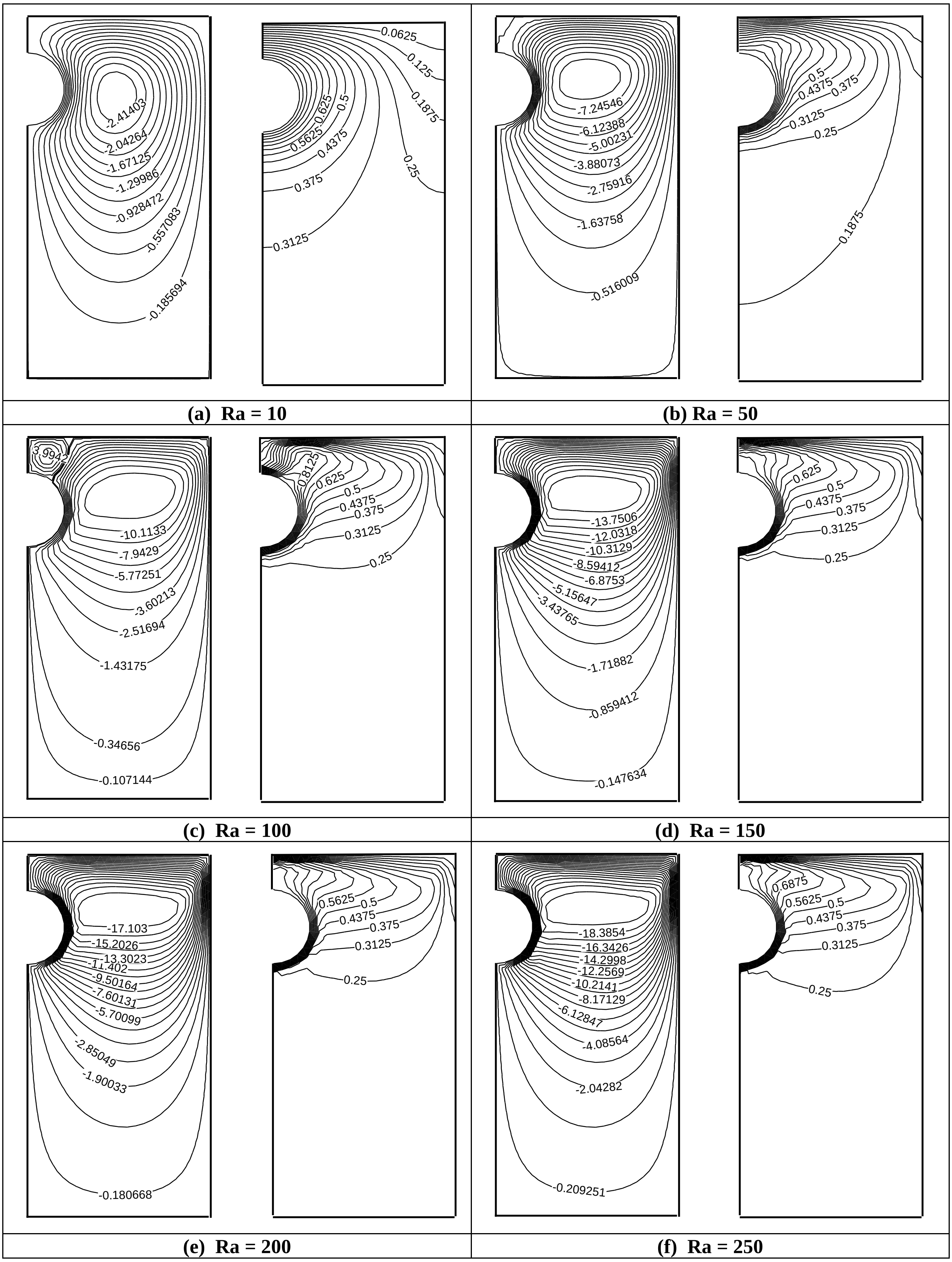

Fig. (3) Streamlines (left) and isotherms (right) around the heated pipe corresponding to h/R=2 and various Rayleigh numbers.

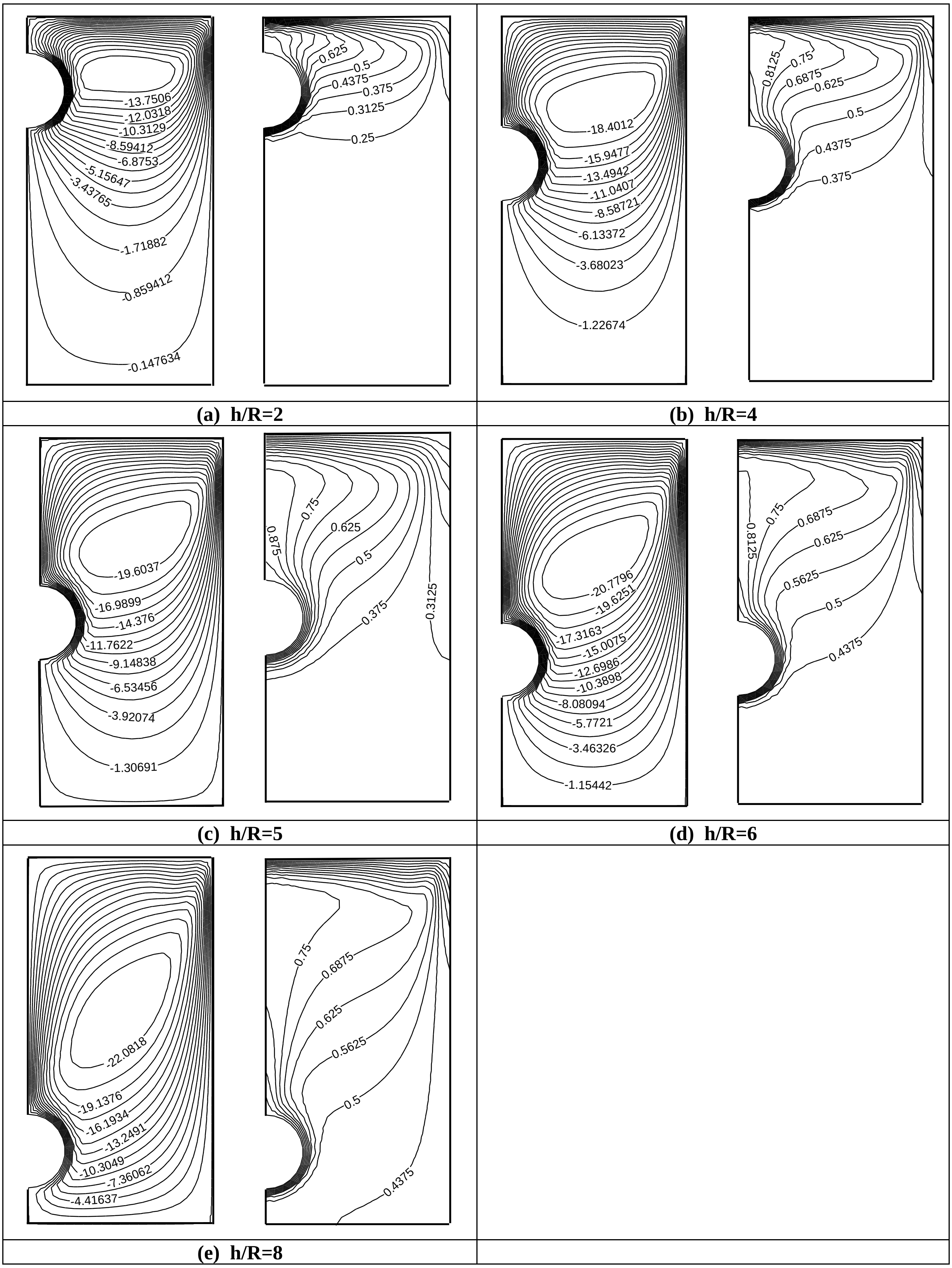

Fig.(4): Streamlines (left) and isotherms (right) around the heated pipe corresponding to Ra=150 and various pipe burial depths .

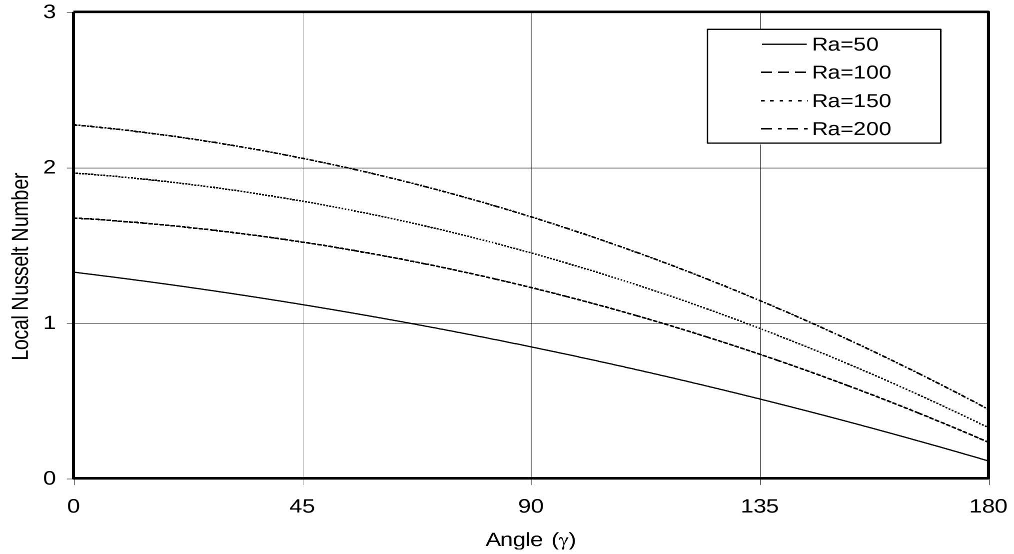

(a) h/R = 3

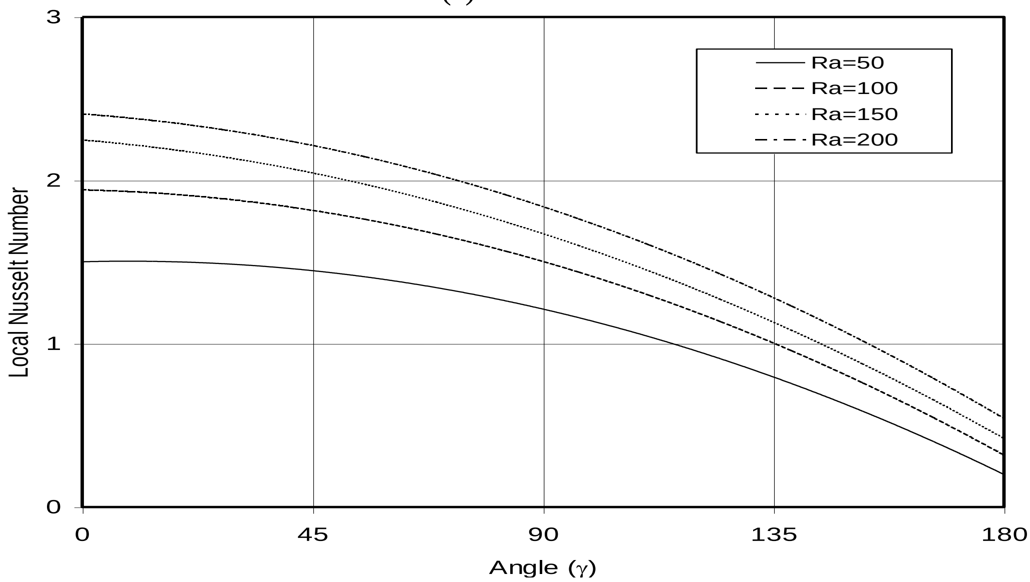

(b) h/R = 5

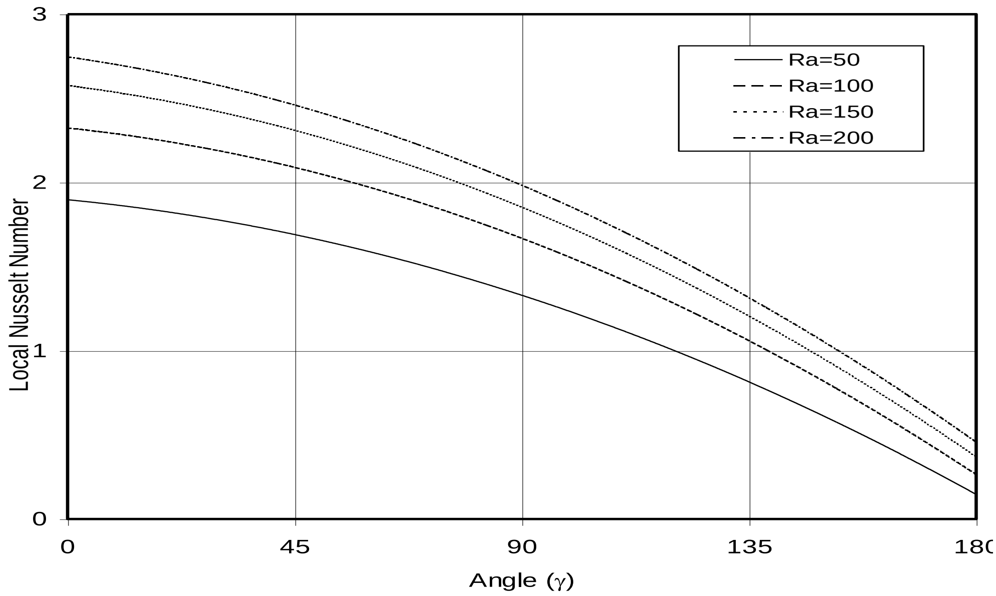

(c) h/R = 8

Fig. (5): Local Nusselt number distribution at various Rayleigh numbers and burial depths

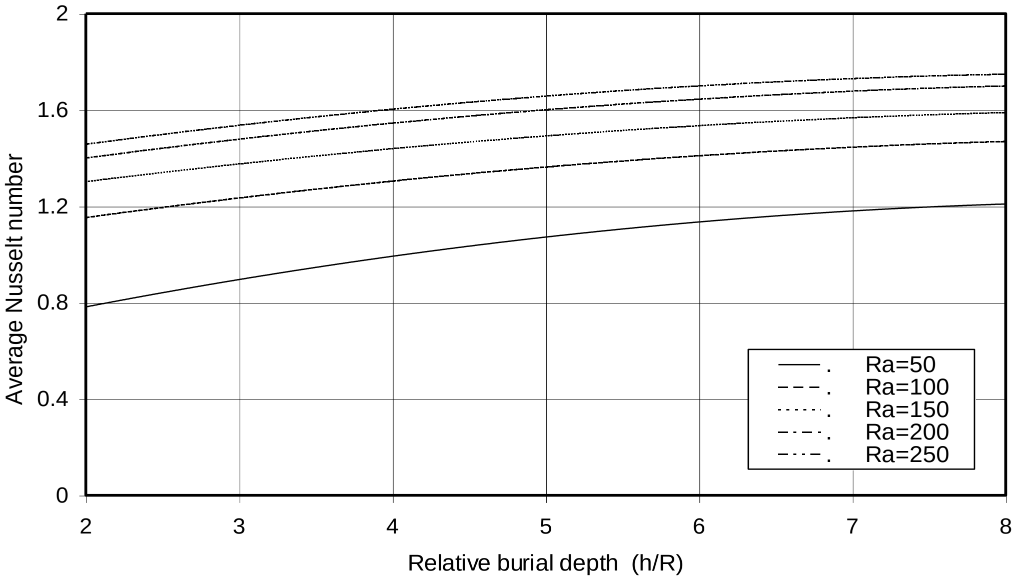

Fig.(6); Predicted average Nusselt number with relative burial depth (h/R) for different Rayleigh numbers

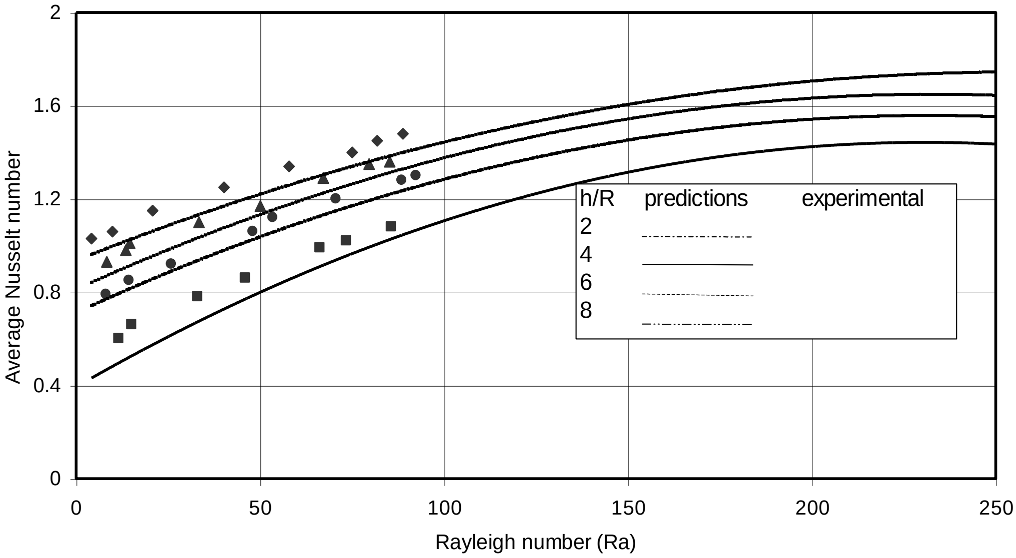

Fig.(7): Comparison of model predictions with experimental results at different burial depths

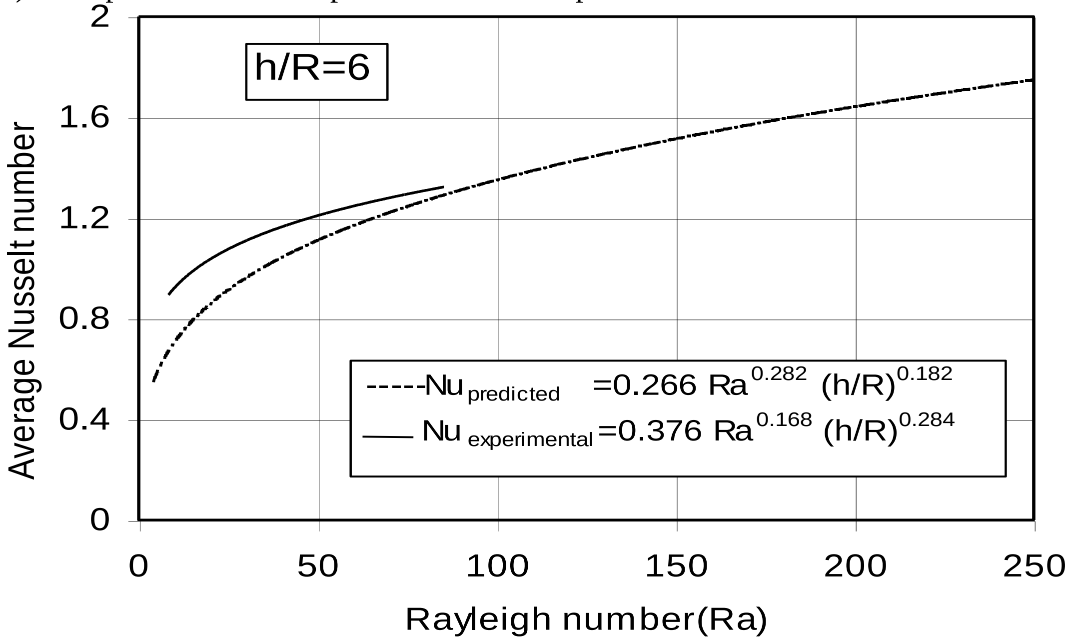

Fig.(8): Comparison between the experimental and the numerical correlations